

# Multi-Hazard Susceptibility Assessment in the Mountainous Regions Using Machine Learning Techniques: A Review

Hemwati Nandan Bahuguna<sup>1</sup>, Sushma Bahuguna<sup>2</sup>  
Syed Hameedur Rahman Zaini<sup>3</sup>, Sudipta Sen Gupta<sup>4</sup>

## Abstract

*Mountainous regions of the world are sites of multiple and overlapping natural hazards that often lead to loss of life, property, and environment. An accurate and timely prediction and assessment of hazardous events can save lives and reduce economic losses in these regions. Multi-hazard susceptibility assessment of mountainous regions may provide holistic valuable insights for effective risk mitigation strategies for future disasters. Currently, Machine learning modeling techniques have enabled novel advances for multi-hazard susceptibility evaluation of natural hazards owing to the availability of the various types of data pertaining to earth observation from multiple sources. Though machine learning modeling techniques have been applied by researchers to provide multi-hazard susceptibility maps for the mountainous regions, building generalized learning techniques of susceptibility and risk evaluation is still a challenge due to the high level of complexity of hazards in these regions. This article contributes a systematic review of machine learning techniques applied by the researchers, especially in the past 10 years for multi-hazard susceptibility assessment in the mountainous regions with adequate contextual information.*

**Keywords:** *Multi-hazard, Machine Learning, Susceptibility, Mountainous Regions, Disaster Management*

---

<sup>1</sup> Hemwati Nandan Bahuguna, Doctoral Scholar, School of Management, GD Goenka University, Gurgaon, India

<sup>2</sup> Sushma Bahuguna, Professor, Tecnia Institute of Advanced Studies, affiliated to Guru Govind Singh Indraprastha University, Delhi

<sup>3</sup> Syed Hameedur Rahman Zaini, Asst. Professor, School of Management, GD Goenka University, Gurgaon, India

<sup>4</sup> Sudipta Sen Gupta, Associate Professor, School of Management, GD Goenka University, Gurgaon, India

## 1. Introduction

Climate change is upon the world and continued unsustainable practices by humans are paving the way to many imbalances. There is an increase in the frequency of natural extreme events worldwide causing great human and environmental losses (Barthel and Neumayer, 2012; Zschau, 2017; GAR, 2022). Over the last 20 years, medium to higher disasters have increased five times higher than disasters reported in the previous three decades and this rapid rise in the frequency of disasters can be attributed to climate change and inadequate risk management (GAR, 2022). Mountainous regions are highly hazardous and natural hazards strike the regions independently, simultaneously, or in a series of cascading events causing huge losses of life (Khatakho et al., 2021; Rusk et al., 2022). UNISDR (2015) report states that between 2005 and 2014, over 70% of the more than seven lac disaster-related deaths occurred in mountainous countries (Rusk et al., 2022). Further, the IPCC report's sixth assessment prediction proclaims multiple changes in many regions due to the changing climate and the incidence of compound hazards may increase multi-hazard risk in mountainous environments (IPCC, 2021).

Since it is difficult to predict coexisting multiple natural hazards, most of the previous studies have focused on assessing individual hazards (Pourghasemi et al., 2017; Javidan et al., 2021). These studies have also neglected the human impacts and the exposure component of natural hazards (Kalantari et al., 2019). Exposure pertains to the situation of people, housing, infrastructure, production capacities, and other tangible human assets located in hazard-prone areas (GAR, 2022). The exposure of communities to hazards can be reduced through an accurate predictive model based on expert analysis, a thorough understanding of influencing factors, and the implementation of mitigation and preparedness measures (Yousefi et al., 2020). Additionally, the effects of hazards can be minimized by adopting new approaches and providing data-driven support for decision-making processes (Michielsen et al., 2016). A wide range of methods namely Opinion driven models, physical-based models, statistical models, and ML models have been applied for hazard susceptibility mapping with advantages and limitations of each of these methods over the other methods (He Qian et al., 2021). Susceptibility is related to spatial aspects of hazard and refers probability of hazard incidences within a selected type during a given location (Azemeraw, 2021). Although single hazard assessments yield insights, they can also lead to ambiguous interactions

between hazards (Kappes et al., 2010; Cutter, 2018). The mitigation strategy of a single hazard in a region may not be definite as one hazard may exacerbate the intensity, frequency duration, and density of another hazard (Kappes et al., 2012; Pouyan et al., 2021). Therefore, it is necessary to integrate studies of the collective likelihood of hazardous events to describe a holistic scenario of hazards in the region (Kappes et al., 2012; Gruber and Mergili, 2013; Karlsson et al., 2017).

The concept of multi-hazard was first introduced by the United Nations in the context of sustainable development and Agenda 21 (UNEP, 1992), with a focus on risk reduction and disaster management as essential components of the planet's sustainable management. Furthermore, it defines the vulnerable areas for multiple hazards with their levels and recognizes priority zones for sustainable development (UN Johannesburg Plan, 2002). Since multiple hazards of a region usually interact with each other and contribute to an overall threat in a complex way (Rocchi et al., 2022), the development of a multi-hazard risk assessment approach is necessary (Schmidt et al., 2011) and is receiving increasing attention (Gruber and Mergili, 2013). Bell and Glade (2004) adopted a general method for multi-hazard analysis of debris flow, rock-fall, and snow avalanches in Iceland. An adaptable software was created by Schmidt et al. (2011) in which researcher was allowed to analyze the natural processes of their concern. Multi-hazard assessment was conducted by Gruber and Mergili (2013) to generate a comprehensive regional scale map for rock slides, ice avalanches, periglacial debris flow, and Lake Outburst flood. Researchers are enhancing natural hazard assessments through the use of Remote Sensing (RS) and Geographic Information System (GIS) technologies (Van Westen, 2013). These tools efficiently identify hazard-prone areas by enabling the collection, storage, combination, manipulation, retrieval, analysis, and visualization of data (Samanta et al., 2018). Recently, Multi-Criteria Decision Making (MCDM) and Machine Learning (ML) methods have gained popularity for multi-hazard analysis and mapping (Bordbar et al., 2022; Cao et al., 2020). Machine Learning, due to its excellent generalization of data and interpretation capacity is more suitable than statistical and MCDM techniques for hazard assessment (Huang et al., 2020).

The machine learning approach plays a significant role in disaster risk reduction by forecasting extreme events, situational awareness, susceptibility and hazard exposure mapping of the events in real-time, and decision support (Kuglitsch et

al., 2022). There is growing recognition of the importance of Machine Learning for effective and informed disaster management that is necessary to address the scale and impact of disaster (Linardos et al., 2022). The ML approach: (i) enables the machine to learn and improve by themselves from experiences of historical events (Barthel and Neumayer, 2012), (ii) can identify patterns and trends in big and complex datasets, and is capable of handling multi-dimensional and multi-variety data from many sources (Pourghasemi et al., 2017; Sarkar, 2021) and (iii) can analyze and map relationship between spatial pattern of historical events and their predisposing factors (Rahmati et al., 2019). Researchers have applied the ML approach for multi-hazard susceptibility assessment in mountainous regions that include ensemble ML algorithms and combining multiple classifiers to have improved results. This article reviews machine learning approaches applied by researchers in the last 10 years for mountainous regions of the world to evaluate models as useful, universal, and accurate multi-hazard mapping products that can be applied by managers and planners.

## 2. Methodology

For this review document, a search was conducted on Google Scholar, Web of Science, and relevant journal databases using the terms “multi-hazard”, “machine learning” “natural disaster”, “disaster management,” “mountainous region” and “case studies” as keywords (Table1), aiming articles published in the period from 2012 to 2022. The search yielded 48 relevant articles excluding review articles. After a manual search based on journal ranking, citation of the articles, and excluding studies outside the scope of the present review, sixteen papers were included in the present review study. The search revealed that an increasing trend of the ML approach about multi-hazard susceptibility in mountainous regions has been initiated by the researcher in recent years.

**Table 1: Keyword combinations used to search the papers included in the review**

Combination No.	Keywords
1	Multi-hazard, machine learning, exposure assessment
2	Multi-hazard, susceptibility evaluation, machine learning
3	Disaster management case studies, machine learning
4	Natural disaster, mountainous region, machine learning
5	Multi-hazard, mountainous region, machine learning

### 3. Literature Review

Multi-hazard susceptibility assessment (MSE) is an initial step of comprehensive risk assessment that can help planners and disaster managers with effective mitigation management (Pourghasemi et al., 2019, 2020). It might be a significant key tool in enhancing resilience and can play an important role in ensuring the long-term sustainability of local ecosystems and communities (Van Westen, 2017). In MSE, data are analyzed to predict the class or category of data points and upcoming events or escalation of an event. Although the methodology and configuration of ML techniques affect the result and performance of the models, different modeling approaches provide valuable information to policymakers and managers to understand the phenomena of the region for effective management of measures (Hill and Minsker, 2010). ML-based multi-hazard susceptibility assessment by the researchers in the mountainous regions of Hindu Kush Himalaya, Iran, Saudi Arabia, Austria, Southeast Asia, Nepal, Italy, and China is summarized in Table 2.

**Table 2: Summary of ML-based multi-hazard susceptibility assessment in the mountainous regions**

S. No.		Dataset	**Conditioning Factors	Performance
1	<p><b>Author:</b> Rusk J. et al., (2022).</p> <p><b>Phenomena:</b> Floods, Landslides and Wildfires</p> <p><b>Area of study:</b> Hindu Kush Himalaya</p> <p><b>*Technique:</b> <i>Maxent</i></p>	<p>Hazard catalog (flood, landslide), VIIRS fire archive, DEM from STRM, CHELSA, FAO-UNESCO, Global Surface Water Explorer, Land Scan data</p>	<p><b>DEM-derived:</b> El, S, A, and flow accumulation</p> <p><b>Meteorological:</b> AMT, AMR</p> <p><b>Surface characteristics:</b> LC and soil suborder</p> <p><b>Hydrological:</b> Distance to permanent water and SM</p>	<p>Area under the receiver operating characteristic curve (AUC) for (Maxent Model)</p> <p>Floods : 0.93</p> <p>Landslides : 0.91</p> <p>Wildfires : 0.86</p>

S. No.		Dataset	**Conditioning Factors	Performance
2	<b>Author:</b> Javidan N. et al., (2021)	Google Earth images, field investigation, water resource organization (national and regional documents), and the Department of Natural Resource Management of Golestan.	<b>Floods:</b> El, Sa, Sp, LU, PC, PrC, TWI, Lth, DD, Stx, DtS, AMR, RSP, TRI, SPI <b>Landslides and Gullies:</b> El, Sa, Sp, LU, PC, PrC, TWI, Lth, DD, Stx, DtS, AMR, RSP, TRI, SPI, DtE, LS factor, DtR	<b>Average AUC for three sample data sets (Maxent Model)</b> Floods : 0.93 Landslides : 0.87 Gully erosion : 0.92
	<b>Phenomena</b> Floods, Landslides, and Gullies			
	<b>Area of study:</b> Gorgan-rood Watershed, Gole-stan province, Iran			
	<b>*Technique:</b> <i>Maxent</i>			
3	<b>Author:</b> Youssef A.M. et al., (2022)	Google Earth images, field investigation applying GPS, national and regional data: civil defense, Jazan region authority, Ministry of Transportation, Saudi Geological Survey, review of technical reports and scientific	<b>Floods:</b> Topography (El, S, TWI PC, A) Climatology (R), Hydrology (DtW, SD), Land cover (LULC NDVI), Geology (Lth), Anthropogenic (DtRd) <b>Landslides:</b> Topography (El, S, TWI PC, A), Hydrology (DtW), Land cover (LULC NDVI), Geology	<b>AUC for Floods</b> RF Model : 0.97 MDA Model : 0.93 FDA Model : 0.94 <b>Landslides</b> RF Model : 0.91 BRT Model : 0.90 GLM Model : 0.92 MDA Model : 0.92 FDA Model : 0.92 <b>Gully erosion</b> RF Model : 0.83 BRT Model : 0.82
	<b>Phenomena:</b> Floods, Landslides and Gully erosion			
	<b>Area of study:</b> Hasher-Fayfa Basin, South-western Saudi Arabia			
	<b>*Techniques:</b> <i>RF, MDA, and FDA</i> <b>Floods:</b> <i>RF, MDA, and FDA</i> <b>Landslides and</b>			

S. No.		Dataset	**Conditioning Factors	Performance
	<b>Gully erosion:</b> <i>RE, BRT, GLM, MDA and FDA</i>	publications.	(Lth, DtF), Anthropogenic (DtRd)  <b>Gully erosion:</b> Topography (El, S, TWI PC, A, TRI, PrC, VD), Climatology(R), Hydrology (SD), Land cover (LULC NDVI), Geo (Lth )	GLM Model : 0.77 MDA Model : 0.73 FDA Model : 0.79
4	<b>Author:</b> Yousefi, S. et al., (2020)  <b>Phenomena:</b> Floods, Landslides, Land subsidence, Snow avalanches and Wildfires  <b>Area of study:</b> Chaharmahal and Bakhtiari Province of Southwestern Iran  <b>* Techniques:</b> <i>SVM, FDA and GLM</i>	Field work, scientific reports, topographic maps, geologic maps, meteorological stations, digital stream layer and piezometric wells	<b>Floods:</b> R, DEM, LU, Lth, S, DtR, NDVI, DtRd, TWI, PC, A, DD  <b>Landslides:</b> DEM, LU, Lth, DtF, S, DtR, DtRd, TWI, PC, A, DD, CI  <b>Land subsidence:</b> DEM, LU, Lth, DtF, S, DtR, GwL, NDVI, DtR, TWI, PC, A  <b>Snow avalanches:</b> DEM, LU, S, PC, A, WEI, TRI, SnD	<b>AUC for Floods</b> SVM Model : 0.97 FDA Model : 0.96 GLM Model : 0.96  <b>Landslides</b> SVM Model : 0.84 FDA Model : 0.77 GLM Model : 0.77  <b>Land subsidence</b> SVM Model : 0.94 FDA Model : 0.92 GLM Model : 0.92  <b>Snow avalanches</b> SVM Model : 0.89 FDA Model : 0.91 GLM model : 0.90

S. No.		Dataset	**Conditioning Factors	Performance
			<b>Wildfires:</b> R, DEM, S, DtR, NDVI, DtRd, TWI, A, T (min), T (max), DtU, WEI	<b>Wildfires</b> SVM Model : 0.83 FDA Model : 0.82 GLM Model : 0.83
5	<b>Author:</b> Nachappa T. G. et al., (2020)  <b>Phenomena:</b> Floods and Landslides  <b>Area of study:</b> Federal State of Salzburg, Austria  <b>* Techniques:</b> SVM and RF	Geological Survey of Austria, incidence of historic flooding, DEM	<b>Floods:</b> EL, S, A, LC, R, Geo, DtRd, DtD, NDVI, TWI, SPI  <b>Landslides:</b> EL, S, A, LC R, Geo, DtRd, DtD, Lit, DtF	<b>AUC for Floods</b> SVM Model : 0.87 RF Model : 0.87  <b>Landslides</b> SVM Model : 0.89 RF Model : 0.90
6	<b>Author:</b> Pouyan, S. et al., (2021)  <b>Phenomena:</b> Flooding, Gully erosion, Forest fires and Earthquakes  <b>Area of study:</b> Kohgiluyeh and Boyer-Ahamad Province, Iran	Google Earth images and field survey supported by GPS, Sentinel Satellite imagery, Google Earth engine	<b>Floods:</b> El, AMR, DtRd, S, LU, TWI, NDVI, DD, PC DtR, Lth, A  <b>Gully erosion;</b> AMR, El, Lth, Stx (sand, silt, clay), DD, DtRd, NDVI, TWI, LU, S, DtR. PC, PrC  <b>Forest fires:</b> AMT, AMR, El,	<b>AUC for Floods</b> SVM Model : 0.94 RF Model : 0.98 BRT Model : 0.88  <b>Gully erosion</b> SVM Model : 0.95 RF Model : 0.99 BRT Model : 0.93  <b>Forest fires</b> SVM Model : 0.72 RF Model : 0.88 BRT Model : 0.68

S. No.		Dataset	**Conditioning Factors	Performance
	<p><b>* Techniques:</b> SVM, RF, BRT and PSHA (for earthquakes)</p> <p><b>* Techniques:</b> SVM, RF, BRT and PSHA (for earthquakes)</p>		<p>DtRd, DtV, NDVI, S, WEI, DtR and TWI, A</p> <p><b>Earthquakes:</b> PGA</p>	
7	<p><b>Author:</b> Rahmati O. et al., (2019)</p> <p><b>Phenomena:</b> Floods Rock falls, and Avalanches</p> <p><b>Area of study:</b> Asara watershed, Alborz Mountains, Iran</p> <p><b>* Techniques:</b> SVM, GAM and BRT</p>	<p>Field survey, documents from road organization of Iran and regional water company</p>	<p><b>Floods:</b> EI, TPI, TRI, TWI, Sd, DtS, PrC, Lth and LU</p> <p><b>Rockfalls:</b> EI, TPI, TRI, LS, RSP, VRM, A, Sd, PrC, Lth and LU</p> <p><b>Snow avalanches:</b> EI, TPI, TRI, LS, RSP, VRM, WEI, A, Sd, PrC, Lth and LU</p>	<p><b>AUC for Floods</b> SVM Model : 0.89 GAM Model : 0.86 BRT Model : 0.94</p> <p><b>Rock Falls</b> SVM Model : 0.93 GAM Model : 0.90 BRT Model : 0.88</p> <p><b>Avalanches</b> SVM Model : 0.92 GAM Model : 0.83 BRT Model : 0.89</p>
8	<p><b>Author:</b> He Qian et al., (2021)</p> <p><b>Phenomena:</b> Landslides and Wildfires</p> <p><b>Area of study:</b> South-east Asia</p>	<p>MODIS, fire archive, global landslide catalog (GLC) SRTM data (DEM), terra climate(climate) OSM, global lithological map</p>	<p><b>Landslides:</b> EI, S, A, PC, PrC, DtR, DtRd, DtF, NDVI, P, SM, Lth, LU, TWI, SPI</p> <p><b>Wildfires:</b> EI, S, DtU, DtR,</p>	<p><b>AUC for Landslides</b> RF Model : 0.89 GBDT Model : 0.87 AdaBoost : 0.86</p> <p><b>Wildfires</b> RF Model : 0.91 GBDT Model : 0.88 AdaBoost : 0.81</p>

S. No.		Dataset	**Conditioning Factors	Performance
	<b>* Techniques:</b> <i>RF, GBDT and AdaBoost</i>		DtRd, NDVI, P, T, TWI and wind speed	
9	<b>Author:</b> Pourghasemi H.R., Gayen, A. et al., (2020)  <b>Phenomena:</b> Floods Landslides and Forest fires  <b>Area of study:</b> Fars Province, Southern Iran  <b>* Techniques:</b> <i>SVM and MARS</i>	ASTER-GDEM, DEM, Geological Survey of Iran, weather stations	<b>Floods:</b> Sa, Al, A, PC, TWI, Geo, LULC, DtR, DtRd, AMR, DD and soil features  <b>Landslides:</b> Sa, Al, A, PC, PrC, Geo, LULC DtR, DtF, DtRd  <b>Forest Fires:</b> Sa, Al, A, TWI, LULC, DtR, DtRd AMT and distance to residential areas.	<b>AUC for Floods</b> SVM model : 0.75 MARS model : 0.76  <b>Landslides</b> SVM model : 0.89 MARS model : 0.91  <b>Forest fires</b> SVM model : 0.91 MARS model : 0.90
10	<b>Author:</b> Pourghasemi H.R., Kariminejad, N. et al., (2020)  <b>Phenomena:</b> Floods, Landslides, and Forest fires  <b>Area of study:</b> Fars Province, Shiraz city, Iran  <b>* Technique:</b> <i>RF</i>	Terrain mapping through field work using GPS, DEM (ASTER-GDEM), river, Google Earth Images, road and urban maps, maps of the Geological Survey of Iran and natural resources,	<b>Floods:</b> Al, Sa, A PC, TWI, DtR, DtRd, DD, Lth,R, LU and soil features.  <b>Landslides:</b> Al, Sa, Sd, PC, PrC, DtR, DtRd, DtF, Lith and LU  <b>Forest fires:</b> Al, Sa, Sd, TWI. DtR, DtRd, DD, DtU, R, AMT	<b>AUC for RF Model</b>  Floods : 0.83 Landslides : 0.93 Forest fires : 0.94

S. No.		Dataset	**Conditioning Factors	Performance
11	<p><b>Author:</b> Khatakho, R. et al., (2021)</p> <p><b>Phenomena:</b> Floods, Landslides, Urban fires and Earthquakes</p> <p><b>Area of study:</b> Kathmandu Valley</p> <p><b>*Techniques:</b> <i>AHP in integration with the GIS</i></p>	<p>Arial photo interpretation, Google Earth engine, survey, historical data, literature review and pilot field observations</p>	<p><b>Floods :</b> S, DtS, LULC, Lth , P, El</p> <p><b>Landslides:</b> DtF, S, A, PrC, DtS, LULC, Lth, DtR, NDVI, P, El</p> <p><b>Fires :</b> LULC, DtR, PD, Distance to (fire brigades, gas station, transmission line, electric substation, main settlement, and old settlement)</p> <p><b>Earthquakes:</b> DtF, S, LULC, Lth, PD, Distance to (old settlement, soil liquefaction, seismic intensity, dominancy building type)</p>	<p><b>For Floods, , landslides and urban fires</b></p> <p>Validation by superimposition of historical hazard events;</p> <p><b>AUC for Earthquake:</b> 0.63, moderate performance 4calculated for the damage due to the 2015 Gorkha earthquake.</p> <p><b>Damage density</b> 0.33 to 0.06</p>
12	<p><b>Author:</b> Rocchi, A. et al., (2022)</p>	<p>Italian National Institute of Statistics (ISTAT) database</p>	<p><b>Building sharing features:</b> building material, period</p>	<p><b>Silhouette coefficient:</b> Good Silhouette</p>

S. No.		Dataset	**Conditioning Factors	Performance
	<p><b>Phenomena:</b> Floods and Earthquakes</p> <p><b>Area of study:</b> Emilia Romagna Region, Italy</p> <p><b>*Techniques:</b> <i>PCA and K-means</i></p>		<p>of construction, state of conversion, superficial extension, number of inhabitants, population density, peak acceleration etc.</p> <p><b>Variables have been grouped into three categories:</b> vulnerability instances, exposure instances and hazard instances</p>	<p>values relative to cauterization.</p> <p>Overall risk label assigned to each cluster confirmed previous risk classification study</p>
13	<p><b>Author:</b> Bordbar M. et al., (2022)</p> <p><b>Phenomena:</b> Floods, Landslides and Earthquakes</p> <p><b>Area of study:</b> Kermanshah Province in Western Iran</p>	<p><b>Floods:</b> Google Earth engine and sentinel - 3 images</p> <p><b>Landslides:</b> historical data and field investigation applying GPS</p>	<p><b>Floods:</b> Al, Sa, Sd, PC, DtR, Lth, R, LU</p> <p><b>Landslides:</b> Al, Sa, Sd, PC, DtR, DtF, dtRd, Lth, LU</p> <p><b>Earthquakes:</b> PGA map</p>	<p><b>AUC for</b> SWARA-ANFIS-PSO ensemble model</p> <p>Floods : 0.93 Landslides :0.89</p>

S. No.		Dataset	**Conditioning Factors	Performance
	<p><b>*Techniques:</b>  <i>Ensemble SWARA-ANFIS-PSO and SWARA-ANFIS-GWO models.</i></p>	<p><b>Earthquake inventory map:</b>                      International Institute of Earthquake Engineering and Seismology</p>		
14	<p><b>Author:</b>                      Pourghasemi H.R. et al., (2019)  <b>Phenomena:</b>                      Floods, Landslides and Earthquakes  <b>Area of study:</b>                      Lorestan Province in Iran  <b>Techniques:</b>  <i>Ensemble SWARA-ANFIS-GWO models.</i></p>	<p>Historical information, field surveys; ASTER-GDEM, Landsat (OLI). Geological Survey of Iran, topographical map, weather stations, agriculture organization</p>	<p><b>Floods and Landslides:</b>                      Al, Sa, Sd, PC, SD, PrC, DtR, DtF, Lth, R and LU  <b>Earthquakes:</b>                      PSHA</p>	<p><b>AUC for SWARA-ANFIS-GWO ensemble model</b>                      Flood : 0.84                      Landslides : 0.80</p>
15	<p><b>Author:</b>                      Cao, J. et al., (2020)  <b>Phenomena:</b>                      Landslides, Rock fall and Debris flow  <b>Area of study:</b>                      Jiuzhaigou region of China</p>	<p>Bureau of land and resources of Sichuan (BLRS), Satellite interpretation in Google Earth</p>	<p><b>Landslides, Rock fall and Debris flow</b>                      Al, A, S, LU, FD, DtR, DtRd, NDVI, AMR, DtF, DtE, and Lth</p>	<p><b>AUC for Landslides SVM Model : 0.88</b>  <b>Rock Falls XGBoost : 0.97</b>  <b>Debris Flow XGBoost : 0.97</b></p>

	<b>*Techniques:</b> <i>SVM, RF and XGBoost.</i>			
16	<b>Author:</b> Zhao, Z.et al., (2022) <b>Phenomena:</b> Landslides and Rock falls <b>Area of study:</b> Hengduan Mountains Region, China <b>*Techniques:</b> <i>SVM, RF and BP NN</i>	On spot visits, natural resources bureaus ASTER GDEM, national Qinghai-Tebet plateau Science data center, open street map	<b>Landslides and Rock falls</b> El, S, A, PC, Lth, DtF, P, NDVI, DtR, and DtRd	<b>AUC for Landslides</b> RF Model : 0.83 <b>Rock falls</b> RF Model : 0.88
<b>Abbreviation Used</b>				
<p><b>*Techniques:</b> AdaBoost; Adaptive Boosting (Freund and Schapire, 1997), AHP; Analytical Hierarchy Process (Saaty, 1988), ANFIS; Adaptive Neuro - Fuzzy Inference System (Jang, 1993) , BPNN; Back Propagation Neural Network (Rumelhart et al., 1986) BRT; Boosted Regression Tree (Friedman, 2001); FDA; Functional Discriminant Analysis (Ramsay and Dalzell, 1991), GBDT; Gradient-Boosted Decision Tree (Friedman, 2002), GAM; Generalized Additive Model (Hastie and Tibshirani, 1986), GLM; Generalized Linear Model (Nelder and Wedderburn, 1972), GWO; Grey Wolf Optimization (Mirjalili et al., 2014), K-Means; K-mean clustering Algorithm (Lloyd, 1982), MARS; Multivariate Adaptive Regression Splines (Friedman, 1991), Maxent; Maximum Entropy (Phillips et al., 2021), MDA; Multivariate Discriminant Analysis (Duda et al., 2001), PCA; Principal Component Analysis (Hotelling, 1933), PSO; Particle Swarm Optimization (Kennedy and Eberhart, 1995), RF; Random Forest (Breiman and cutler, 1993), SVM; Support Vector Machine (Cortes and Vladimir, 1995), SWARA; Stepwise Weight Assessment Ratio Analysis (Kersulienė and Turskis, 2011), XGBoost ; Extreme Gradient Boosting (Chen and Guestrin, 2016).</p>				

**\*\*Conditioning Factors:** A; Aspect, Al; Altitude, AMR; Annual Mean Rainfall, AMT; Annual Mean Temperature, CI; Convergence Index, DD; Drainage Density, DEM; Digital Elevation Model, DtD; Distance to Drainage, DtE; Distance to Epicenter, DtF; Distance to Faults, DtR; Distance to Rivers, DtRd; Distance to Roads, DtS ; Distance to Stream, DtU; Distance to Urban, DtV; Distance to Villages, DtW; Distance to Wadis, El; Elevation, FD; Fault Density, Geo; Geology, GwL; Ground Water Level, H; Humidity, Lth; Lithology, LC; Land Cover LU; Land Use, LULC; Land Use and Land Cover, LS; Length Slope, NDVI; Normalized Difference Vegetation Index, P; Precipitation, PC; Plan Curvature, PD; Population Density, PrC; Profile Curvature, PGA ; Peak Ground Acceleration, PSHA; Probabilistic Seismic Hazard Analysis, R; Rainfall, RSP; Relative Slope Position, S; Slope, Sa; Slope aspect, Sd; Slope degree, SD; Stream Density, SG; Slope Gradient, SM; Soil Moisture, SnD; Snow Depth Sp; Slope percent, SPI; Stream Power Index Stx; Soil texture, ST; Soil Types, T; Temperature, TPI; Topographic Position Index, TRI; Terrain Ruggedness Index, TWI; Topographic Wetness Index, VD; Valley Depth, VRM; Vector Ruggedness Measures, WEI; Wind Exposition Index, WS; Wind Speed.

### 3.1 Machine Learning Techniques

Machine learning techniques comprise a group of computational algorithms that learn from historical data, build predictions and classification models, and predict the output whenever it receives new data. ML Algorithms can be broadly classified into three groups namely Supervised ML, Unsupervised ML, and Reinforcement learning. Supervised ML models are trained with labeled data sets, which allow the models to learn and grow more accurately over time. In Unsupervised, ML algorithms learn from the unlabeled data and find the hidden patterns in the data. Reinforcement machine learning trains machines through trial and error to take the best action by establishing a reward system. In hazard susceptibility assessment, the ML approach learns and analyses the relationship between the spatial pattern of historical events and the spatial pattern of the conditioning factors influencing their likelihood (Pourghasemi et. al., 2019). An overview of ML workflow for hazard susceptibility is depicted in Figure 1. The performance of the machine learning approach for an

assigned task is established based on the availability of sufficient quality data and the selection of the right model architecture. **Different ML modeling techniques applied by the researchers for MSE in mountainous regions are mentioned in Table 2.**

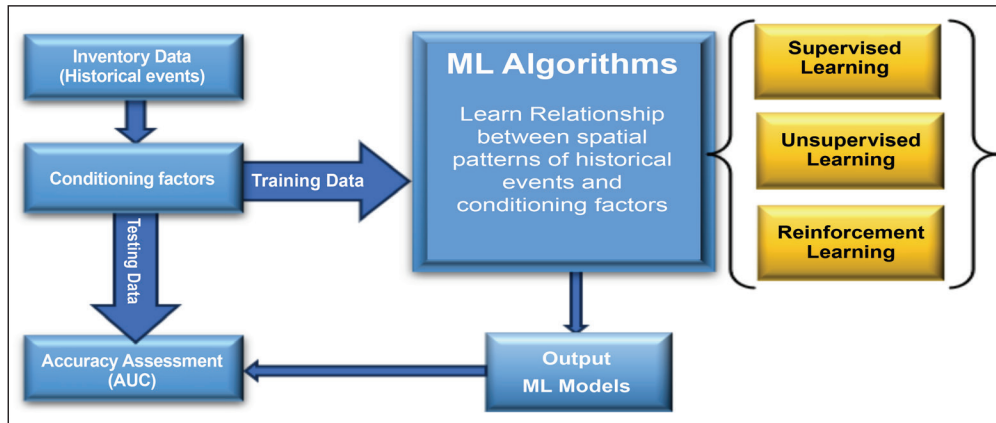


**Figure 1: Overview of machine learning workflow for hazard susceptibility**

### 3.2 Hazard Inventory

Preparation of Hazard Inventory of landforms by recording the location of disaster occurrences is a key step for susceptibility mapping (Javidan et al., 2021). ML is a data-driven technology and the accuracy of predicted output depends on the quality and amount of data. Therefore, it is imperative to have a good set of inventories for improved modeling and mapping. Data generation of events primarily depends on the scale of study, purpose of the study, and accessibility to the study area. Earth observation data provides critical input for machine learning models that improve hazard prediction, detection, and management, ultimately mitigating the impacts of natural disasters. Earth observation data sources can be categorized based on the platform, sensor type, temporal frequency, and spatial resolution. Satellite-based remote sensing provides various data types, such as optical, radar, thermal, and multispectral imagery. These data sources provide geospatial, environmental, climatic, and socio-economic data, which are essential to develop accurate hazard models. Key satellites include Landsat for long-term land monitoring, Copernicus Sentinel satellites for high-resolution optical and radar data, World View Satellites for damage analysis

and land cover change, and Terra SAR-X for terrain monitoring. Airborne sensors like drones can capture detailed local-level data for rapid hazard response. The advantages of ground-based sensors include real-time observation capability, but are localized by space. Earth observation data spans a range of spatial and temporal resolutions, from meters to kilometers and daily to annual intervals.

The data sources used by the researchers for multi-hazard susceptibility mapping include hazard catalog, Visible Infrared Imaging Radiometer Suite (VIIRS) fire archive, Shuttle Radar Topography Mission (SRTM), CHELSA (Climatologist at High Resolution for the Earth's Land Surface Areas, Food and Agriculture Organization (FAO) and United Nations Educational, Scientific and Cultural Organization (UNESCO), Google Earth, Sentinel-2, Moderate Resolution Imaging Spectroradiometer (MODIS), Advanced Spaceborne Thermal Emission and Reflection Radiometer (ASTER) Global Digital Elevation Model (GDEM), Operational Land Imager (OLI), United States Geological Survey (USGS), Global surface water explorer, Geological maps, topographical maps, open street map, weather station, seismic stations, and meteorological stations.

### 3.3 Conditioning Factors

Conditioning factors are essential for hazard susceptibility mapping and modeling (He Qian et al., 2021). Integration of hazard inventory data and the development of a dataset of conditioning factors is a crucial part of multi-hazard susceptibility assessment. Since each mountainous region has a unique geotectonic and hydrologic setting, there is no uniform list of conditioning factors of each hazard (Rahmati et al., 2019). Therefore, researchers have selected conditioning factors based on literature review, expertise towards phenomena, topographical, geological, hydrological, climatological, anthropogenic characteristics of the study area, and scale of analysis. Ideally, the selected conditioning factors should be operative, quantifiable, and non-uniform (Nacchapa et al. 2020). Some of the studies have used variance Inflation Factors (VIF) and tolerance (TOL) for multicollinearity tests and Random Forest (RF), Mean Decrease Gini (MDG), and Buruta algorithm for priority of effective conditioning factors. Jackknife test is also used to assess the relative strength of each predictor variable in some studies. Conditioning factors of each hazard applied for multi-hazard modeling by the researcher have been listed in Table 2.

### 3.4 Accuracy Assessment

The area under the receiver operating characteristic curve (AUC) is the most commonly used threshold-independent method for analyzing the performance of the ML models (Marzban, 2004). The goodness-of-fit and predictive performance of ML models are evaluated by using the training group and validation group of data respectively. The receiver operating characteristic (ROC) curve is a plot of sensitivity vs. “1 - specificity” of an investigative test.

$$\text{Sensitivity} = \text{TP} \div \text{TP} + \text{FN}$$

$$\text{Specificity} = \text{TN} \div \text{FP} + \text{TN}$$

Where True positive (TP), True negative (TN), False positive (FP), and False negative (FN) are the fundamental elements of the confusion matrix.

Sensitivity and specificity represent the probability of correct predictions of the positives and negatives as observed in reality (Pourghasemi et al., 2020). AUC values vary between 0 to 1, where 0 implies a completely inaccurate test and 1 infers a perfect accuracy of the test. While classifying model accuracy, an AUC value under 0.7 is unacceptable, 0.7 to 0.8 is considered good, 0.8 to 0.9 is measured as very good, and more than 0.9 is excellent (Swets, 1988; Tien et al., 2017).

Other accuracy measures applied by researchers to evaluate the performance of the multi-hazard models are as follows:

- (i) **Overall accuracy (ACC)** =  $\text{TP} + \text{TN} \div \text{TP} + \text{TN} + \text{FP} + \text{FN}$   
(Measures the percentage of correctly classified samples)
- (ii) **True skill statistics (TSS)** =  $\text{sensitivity} + \text{specificity} - 1$   
(Measures the ability of a predicted value to discriminate between the events and nonevents using all the elements in the confusion matrix)
- (iii) **Precision** =  $\text{TP} \div \text{TP} + \text{FP}$   
(Measures of exactness indicating the percentage of samples predicted as positive are exactly positive)
- (iv) **Corrected classified instances (CCI)** =  $(\text{TN} + \text{TP} \div (\text{TN} + \text{TP} + \text{FP} + \text{FN}) * 100$   
(Considers TN and FN for true and false negative predictive events, and TP and FP for true and false positive, respectively)

(v) **Gini coefficient** =  $2 * AUC - 1$

(Measures the inequality among values of variable and evaluates the performance of binary classifier models)

- (vi) **Silhouette coefficient:** Silhouette score is a measure of accuracy for classified observation and represents object similarity to its cluster compared to other clusters. Its value ranges from -1 to +1, where a high value shows that the object is well-matched to its cluster and poorly matched to neighboring clusters. Euclidean distance and Manhattan distance metrics can be used to calculate silhouette. The disadvantage of the reliability of the approach in the silhouette method is the dependency on the existence of valid quantitative initial data of the region (Rocchi et al., 2022).

### 3.5 Multi-Hazard Susceptibility Modeling

To explore population exposure to multi-hazard risks (landslides, floods, and wildfires) across the Hindu Kush Himalaya, the maximum entropy ML technique was applied by Rusk et al. (2022). A set of 10 environmental covariates was employed to build Maxent models for each hazard. The covariates included meteorological (annual temperature and annual precipitation), surface characteristics (land cover and soil suborder), hydrological (soil moisture and distance to permanent water), and DEM-derived factors (elevation, slope, aspect, and accumulation). Variance inflation factors (VIF) were used to perform a test of multicollinearity and Pearson's correlation coefficient was applied to determine the nature of the correlation. AUC reported single hazard model performance of test data as 0.93 for floods, 0.91 for landslides, and 0.86 for wildfires. Exposure was determined by a multi-hazard susceptibility map integrated from three hazard maps and population distribution data. Javidan et al. (2021) also presented the Maxent ML technique to generate susceptibility maps for landslides, floods, and gullies in the Gorganrood watershed of Iran. Seventeen Geo-geo-environmental factors were selected as predictors for flood, landslides, and Gully erosion. VIF and Tolerance (TOL) were applied for the multi-collinearity test and sensitivity analysis was implemented to examine the relative strength of predictor variables using the Jackknife test. The most influencing predictors for each hazard were considered as; (i) river density, distance from stream, and elevation for floods; (ii) elevation, lithology, and annual mean rainfall for landslides and (iii) annual

mean rainfall, elevation, and lithology for gully erosion. The accuracies gained by the validation model based on AUC values for floods and landslides are comparable to the results of the Maxent model of Rusk et al. (2022).

Yousefi et al. (2020) proposed SVM, GLM, and FDA methods to address the probabilities of landslides, land subsidence, floods, snow avalanches, and wildfire hazards for the mountainous region in southwestern Iran. For this purpose, effective factors were classified into five categories namely topography, geology, hydrology and climatology, social, and vegetation/land cover. Models of each hazard with high accuracies were integrated using Boolean algorithms based on low, moderate, high, and very high classes of each hazard. SVM provided the best accuracy for the prediction of landslides, floods, and land subsidence. GLM predicted the best accuracy for wildfire and FDA generated the best results for snow avalanche risks. Youssef et al. (2022) worked to map the probabilities of landslides, floods, and gully erosion hazards using GLM, FDA, MDA, RF, and BRT models in the Hasher-Fayfa Basin of southwestern Saudi Arabia. Five ML models (GLM, FDA, MDA, RF, and BRT) for landslide and gully erosion and three models (FDA, MDA, and RF) for floods were developed to evaluate hazard occurrences. Based on the literature review topographical, geological, meteorological, hydrological, and anthropogenic factors were incorporated to develop a multi-hazard risk model. Sixteen factors (11 factors for landslides, 12 factors for floods, and 13 factors for gully erosion) were selected to generate hazard susceptibility maps. VF and TOL were used for multicollinearity whereas the RF algorithm was implemented to measure the importance of independent indicators for their contribution to each hazard modeling. FDA model produced the best results for predicting landslides and the RF model provided the best results for predicting floods and Gully erosion. FDA model reported better predictive ability for landslide prediction and lesser predictive ability for flood prediction as compared to the FDA model of Yousefi et al. (2020).

Random Forest model yielded high predictive accuracies for multi-hazard modeling by Nachappa et al. (2020) and Pouyan et al. (2021). Nachappa et al. (2020) produced a multi-hazard exposure map using SVM and RF for landslides and flooding in the Federal State of Salzburg, Austria. Multi-hazard exposures were recognized using a total 13 influencing factors (10 factors for landslides and 11 factors for floods). A quartile

classification approach was applied to categorize the exposure map into five classes of exposure levels. The approach allocated all the values into clusters that contain an equal number of values for better classification compared to the natural break classification approach. The accuracy assessment of the exposure maps was derived through ROC and R-Index (relative density). RF model yielded better performance for both landslides and floods. Pouyan et al. (2021) developed SVM, RF, and BRT models to produce a multi-hazard map for flood, gully erosion, forest fire, and earthquake in Kohgiluyeh and Boyer-Ahmad Province, Iran. The earthquake hazard map was generated from a probabilistic seismic hazard analysis and PGA values were divided into low moderate and high classes. The mean decrease Gini (MDG) method was applied to examine the relative importance of effective factors of each hazard. Elevation was measured most important factor for flooding, whereas annual temperature and mean annual rainfall were measured as the most important factor for forest fire and gully erosion respectively. Aspect was ascertained least important factor for all three hazards. The RF model outperformed other classifiers with AUC Values of 0.99, 0.99, and 0.88 for gully erosion, flooding, and forest fires respectively. The SVM model provided better accuracies for flood predictions than the SVM models of Nachappa et al. (2020) and Rahmati et al. (2019).

Rahmati et al. (2019) proposed SVM, BRT, and GAM for rock fall, avalanche, and flood hazards in the mountainous area of the Asara watershed, Iran. Fourteen predictive factors (topo-hydrological, geo-environmental, and morphometric) were selected for hazard susceptibility mapping based on a literature review. The hazard susceptibility map of each disaster was integrated using the weight linear combination (ELC) technique to produce a multi-hazard map. TSS and AUC were used to evaluate the model performance of each hazard. The SVM model achieved the highest accuracy for snow avalanches and rock falls while the BRT model established the highest accuracy for flood hazards. Proximity to residential areas, road networks, and power transmission lines was defined as a vulnerable component for exposure mapping. AHP was used to determine the weight of each factor and five classes of exposure from very low to very high exposure were assigned. Exposure and multi-hazard maps were assigned risk equation ( $\text{Risk} = \text{Hazard} * \text{Exposure}$ ) to produce a multi-hazard exposure map of the region.

He Qian et al. (2021) studied the intersection of landslides and wildfires using RF, AdaBoost, and GBDT ensemble ML algorithms in Southeast Asia. Fifteen factors for landslides, ten factors for wildfires, and a total of eighteen conditioning factors were chosen for the hazard susceptibility assessment based on information collected from the literature. VIF and TOL were used to detect the quantity of multicollinearity and the mean decrease Gini Index of RF was applied to determine the relative importance of the variables. For landslides, distance to road and distance to faults were considered the most important factors whereas distance to urban areas followed by distance to roads and slopes were considered the most important factors for wildfires. The model performance was evaluated using (ACC), Precision, AUC, and confusion matrix values. RF model outperformed other classifiers for both landslide and wildfire prediction. The authors also computed the coefficient of variation (CV) for the reliability test by intersecting the susceptibility map with uncertainty.

Pourghasemi, Gayen et al. (2020) developed individual and collective multi-hazard risk maps for floods, landslides, and forest fires using the SVM and MARS, models in Fars province, Southern Iran. The sixteen conditioning factors identified by the literature review were considered to model the risk distribution for floods, landslides, and forest fires. The performance of the models for each hazard was evaluated by AUC, TSS, and correlation and deviance values from each model for each hazard. The AUC values of the MARS model were slightly better than the SVM model for floods and landslides whereas the SVM model performed slightly better than MARS for forest fires. The TSS values depict better landslide prediction by the MARS model but were less able to predict flood and forest fire risk patterns.

Pourghasemi, Kariminejad et al. (2020) conducted a multi-hazard probability assessment using RF classifier for landslides, floods, and forest fires hazards in Fars Province, Iran. The influencing factors were divided into biophysical and human categories. The biophysical category was divided into atmospheric (humidity, rainfall, and temperature) and topographic factors (altitude, slope aspect, and slope degree). The human factors included land use, access to the forest, and fuel management processes. To evaluate the importance of effective factors controlling hazard locations, 12 factors for floods and 10 factors each for landslides and forest fires were selected. Boruta algorithm was applied to prioritize the impact of each respective factor on

the occurrence of each hazard. Susceptibility maps of each hazard were integrated to produce a multi-hazard probability map. The AUC values for validation were reported as 0.83, 0.93, and 0.94 for flood, landslide, and forest fire prediction respectively. Other accuracy measures i.e. sensitivity, specificity, CCI, TSS, and Gini coefficient also approved the AUC results.

Khatakho et al. (2021) developed AHP in integration with GIS to assess multi-hazard risk in Kathmandu Valley for floods, landslides, earthquakes, and urban fire hazards. Multi-hazard risk assessment was performed by pair-wise comparison of floods, landslides, earthquakes, and urban fire hazards. Twenty-one influencing factors were selected based on available information and a suitable class of influencing factors and corresponding rating factors were assigned. Individual maps were generated by selected influencing factors and thereafter four maps were superimposed based on their weights to generate multi-hazard risk map. AUC and hazard density were used to validate the earthquake hazard map based on damage data from the 2015 Gorkha earthquake. While an AUC value of 0.68 reported moderate performance, hazard density analysis illustrated a good correlation between classified hazard zones and past earthquake incidences. Validation for floods, landslides, and urban fire hazards was carried out by superimposing historical hazard events.

Rocchi et al. (2022) presented qualitative multi-hazard risk analysis methodology with large and heterogeneous input data sets to assess overall combined seismic and hydraulic risk for different municipalities of the Emilia Romagna region of Italy. The input dataset of the Italian National Institute of Statistics (ISTAT) was organized as a matrix with rows of municipalities and columns corresponding to quantitative variables associated with different characteristics of flood and seismic risk. PCA method was used to quantify the relative importance between variables and the relation among them. The different municipalities of the region were grouped into homogeneous clusters through the K-mean clustering algorithm and the Silhouette coefficient was used to validate the clusterization.

Pourghasemi et al. (2019) proposed a SWARA-ANFIS-GWO ensemble model in the Lorestan province of Iran for a multi-hazard probability map of landslide, flood, and earthquake. Eleven influencing factors related to terrain and land use were adopted to generate susceptibility maps of landslides and flood. Probabilistic seismic hazard

analysis (PSHA) was employed to generate an earthquake map with 5 different classes from very high to very low based on magnitude. SWARA approach was applied for weighing contributing factors whereas the ANFIS method was implemented to acquire weights on each value while using the GWO algorithm. The AUC indicated accuracies of 84% and 80% for floods and landslides respectively. Multi-hazard probability map was produced by combining landslide, flood, and earthquake maps. Bordbar et al. (2022) also worked on ensemble SWARA - ANFIS - GWO and SWARA - ANFIS - PSO models to provide a multi-hazard map for floods, landslides, and earthquakes in Kermanshah province of western Iran. Influencing factors were selected based on previous research. Altitude, lithology, slope degree, distance to river, plan curvature, and aspect were considered common factors for flood and landslide mapping. Rainfall and land cover for floods and distance to road, distance to fault, and land use were considered as specific influencing factors for landslides. VIF and TOL were used to examine multicollinearity. The SWARA method was applied to weigh the subclass of the influencing factors for landslides and floods. ANFIS, ML algorithm was used in combination with PSO and GWO meta-heuristic algorithms to train the data. A PGA map was generated to study earthquakes in the region. The hazard accuracy of the models was validated using ROC, root mean square Error (RMSE), and mean square error (MSE) methods. SWARA-ANFIS-PSO ensemble models performed best for flood susceptibility maps and provided excellent results for landslide maps. The model reported better accuracies than the SWAEA – ANFIS - GWO ensemble model of Pourghasemi et al. (2019) for predicting floods and landslides.

Zhao et al. (2022) developed and compared six models using three ML methods namely SVM, RF with different nuclear functions, and BPNN model for landslide and Rockfall hazard susceptibility in the Handgun mountains region of China. They adopted 10 factors in susceptibility assessment based on mean decrease Gini and mean decrease indicators by the RF model. RF model provided the highest accuracy compared to other models considered in the study. Cao et al. (2020) implemented SVM, RF, and XGBoost techniques to generate a multi-hazard susceptibility map for landslide, rock fall, and debris flow in the Jiuzhaigou region of China. For this purpose, multi-hazard inventory from 2000 to 2015 was used along with 12 factors associated with triggering mechanisms as conditioning factors. XGBoost performed best for rock fall and

debris flow whereas SVM provided the best prediction for landslides. XG Boost model also reported better accuracy than the RF model of Zhao et al. (2022) for rock fall prediction.

#### **4. Discussion**

Multi-hazard susceptibility modeling worked out by researchers in different mountainous regions of the world reveals that models differ in their accuracy of prediction for different hazards and the type of hazard can affect the ranking of the model. In most of the studies individual hazard susceptibility models were created using different ML algorithms including ensemble methods, and multi-hazard susceptibility maps were assembled from the most accurate individual model for each hazard. Figure 2 depicts the performance of individual ML Models based on AUC Values (Table 2) calculated by researchers for different hazards in the mountainous regions. The Random Forest model (AUC= 0.97, 0.87, 0.98) performs excellently in some tests but exhibits variability in others when predicting floods. The SVM model also exhibits greater variability, with one notably low result of AUC (0.75) for flood prediction. The FDA demonstrates strong overall performance, though it can struggle with certain data, achieving an AUC of 0.77 for landslide prediction. The SVM is highly variable, with AUC ranging from 0.91 to 0.72, suggesting that the performance of this model might depend on the particular subset of data or class distribution for wildfire prediction. The BRT model is highly variable, with an excellent AUC of 0.93 and a poor AUC of 0.63, which may suggest that it will not be good at some subsets of the data for gully erosion prediction.

Mapping processes have the significant disadvantage of being sensitive to changes in input variable weighting and the researcher's judgment on the assessment scale (Chang et al., 2008). All the methodologies have their advantages and limitations, and each model's performance depends on the input data, structure, and accuracy of the model. There is neither a standard for a specific model to be used for a specific situation, hazard, or study area nor universal guidelines on choosing influential factors for each natural hazard (Khosravi et al. 2018).

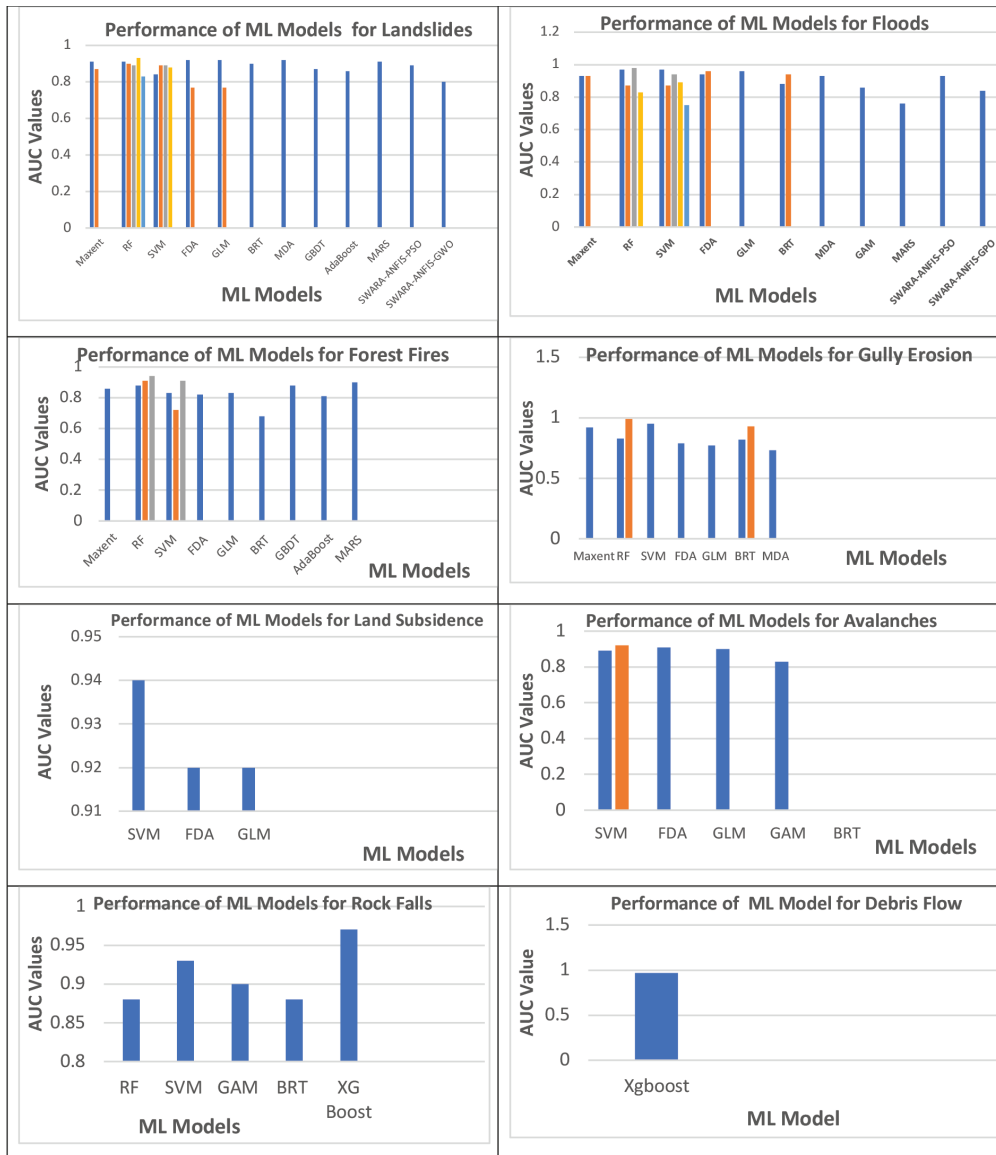


Figure 2: Bar Plots showing the performance of individual ML Models for different hazards

Natural hazards are complex phenomena and have a strong relationship with the characteristics of the landscape (Geotectonic, hydrologic, climatic etc.) and anthropogenic activities of the region. An accurate knowledge of factors affecting these hazards may be incomplete and some of unknown factors may still be present. To assess the performance of various models, relative and proportional research is necessary for similar conditions and influencing factors to make comparisons and rational conclusions on the appropriate model for a specific hazard at a certain region (Goetz et al., 2015). The performance of the models is determined by data sets of historical environmental processes but the reshaping of the environment due to anthropogenic, climate change and urbanization may reshape the distribution of future hazards (IHCAP, 2017; Mukherji et al., 2018; Sharma et al., 2019).

Natural hazards do not operate in isolation and hazard interactions and interaction network modeling are necessary as the occurrence of primary hazard can significantly modify the probability of secondary hazard (Gill and Malamud, 2016). Machine learning models are not definite about the mechanisms giving rise to multi-hazard. Single-hazard and multi-hazard environments differ by mechanistic connection between hazards and one hazard may compound the effects of another hazard (Cutter, 2018). Although a hazard interaction matrix has been given by Kappes et al. (2010) to identify the influence of one hazard on another, but compound effect is somewhat more complex due to various geological, geographical, hydrological, seismic, and anthropogenic processes of the region. Gill and Malamud (2016) suggested that management priorities could be distorted if interactions between important environmental and anthropogenic processes are ignored and considering interactions helps us for better prioritization of resources for disaster risk reduction. Integration of hazard interaction aspects in the multi-hazard modeling approach can contribute to a better holistic assessment of the hazard risk of the region.

Mountain regions are habitat to 17% of the world's population, most of which are poor and marginalized (UNISDR, 2010). Assessment of exposure needs to be interpreted into risk assessment with the help of additional data on social vulnerability within the population (Rigg et al., 2016). The adaptive capacity of different social groups may make substantial differences in vulnerability to hazards among different population sections. For instance, poverty may be the reason for settlement in high-risk areas (Tuladhar et al., 2015) causing increased vulnerability to multiple hazards.

Each disaster type is unique, and each mountainous region has diverse vulnerabilities and resiliency levels. Multi-hazard susceptibility and exposure analysis approach is a cost-effective engineering that can assist the population in adapting to hazardous events. Integrated multiple hazard interaction data capture techniques are necessary in the domain of multi-hazard susceptibility and exposure assessment to develop clean and big structured data that can support the ML approach for improved results. With hazard interactions and networks being integrated with vulnerability and exposure factors along with other important features like the effects of climate change on multi-hazards, remote sensing and earth observation data, socio-economic and infrastructure vulnerabilities, resilience and adaptive strategies, real-time data assimilation, public awareness and an interdisciplinary approach, a treasure trove of valuable insights can be gained. These knowledge inputs can improve disaster preparedness and mitigation measures in the mountainous regions through better hazard prediction, optimizing resource allocation, promoting sustainable land use, and strengthening community resilience.

## Challenges

One of the major challenges for multi-hazard susceptibility assessment is that of building generalized learning techniques by understanding and applying integrated interaction matrices between multiple hazards in learning algorithms. Besides, the availability and collection of data on hazard interactions and interaction networks with correct sampling and sufficient representation of each pattern of hazards is a challenge. ML algorithms require correctly sampled training data having sufficient representation of patterns for the statement of the problem to be merged in the data server. The ML approaches are processed as an integrated approach and may also face challenges related to personal privacy risk and country-specific data leading to limitation of data availability (Kuglitsch et al., 2022). Another data-related challenge relates to ethical concerns. Socio-economic biases in the data sets could not be disseminated through the models developed by the system. Possible harms associated with ML, such as underrepresentation due to human or technical bias should be mitigated and the assistance of ML can be recognized for all, particularly those who are more vulnerable to the impacts of hazards (Kuglitsch et al., 2022). Ensuring unbiased and ethical machine learning tools applied to the ML approach for disaster risk management is one of the

important traits (Rocchi et al., 2022). Mellowed machine learning tools should not be used in safety-critical situations for which they are not prepared (Gevaert et al., 2021). We obtain huge amounts of data from different sources for research applicability and ethics should be carefully considered and misuse should be avoided (Gevaert et al., 2021; Wagenaar et al., 2020; Stahl, 2021). The ethical issues include malicious use, loss of human decision-making, prioritization in risk management, and prioritization of the wrong problems concerning the expectations of stakeholders (Rocchi et al., 2022). The clusterization labeling should be essentially filled with the intention of the end user (Stahl, 2021).

While publicizing results, sensitive aspects should be kept in mind from the privacy point of view (GFDRR, 2018). The results must be humanly explicable and acceptable but this can be challenging as there is no general out-of-the-box human-machine interface that delivers evidence about how and why certain decisions are made by the ML model. Ultimately, faith in timely and fully transparent communication tools is the major challenge to be overcome. This requires effective collaboration among skillful disaster responders, ML developers, geoscientists, regulators, and government agencies, to meet the necessities of all stakeholders. Expertise in communicating results, uncertainties of machine learning, and identification of sensitive groups for overcoming bias are other significant aspects. So, before being applied it is essential to confirm promising results and assessment proneness of tools (Rocchi et al., 2022; Gevaert et al., 2021).

## 5. Conclusion

Mountainous regions are highly prone to a variety of nature-triggered disasters affecting the lives of millions of people worldwide each year. There is a great need to assess hazards holistically which may be helpful to manage the potential threats of these regions. The multi-hazard approach supports the holistic susceptibility assessment of the hazard potential of a particular region that can assist disaster management operations to prepare collectively for the greater risk from multiple hazards. In this article, a review study has been carried out to explore the machine learning models applied by researchers for multi-hazard susceptibility assessment in different mountainous regions of the world.

The performance evaluation of the models reveals that RF, FDA, GLM, Maxent, and MDA consistently deliver the highest AUC values for flood and landslide prediction. Random Forest stands out as the most reliable and effective model for wildfire prediction,

with SVM and Maxent also demonstrating strong potential. For gully erosion prediction, Maxent and Random Forest are the most effective models. In terms of land subsidence prediction, both SVM and GLM are excellent options, with SVM slightly outperforming GLM. For snow avalanche prediction, GLM and BRT yield good results while XGBoost achieves exceptional accuracy for rockfall and debris flow prediction. The machine learning methods achieved acceptable accuracy in predicting the different hazard types and multi-hazard susceptibility maps are generated by the researchers to provide useful information for proactive management and hazard mitigation.

Future research on the integration of hazard interaction aspects and interdisciplinary approach combining data science, engineering, environmental science, social science, and policy studies into multi-hazard modeling can contribute to an enhanced framework for disaster risk reduction. Further, the exploration of strategies for building generalized learning models and methods for improved accuracy can expand disaster management procedures in mountainous regions.

## References

1. Azemeraw, W.A. (2021). Landslide Inventory, Susceptibility, Hazard and Risk Mapping. In book: *Landslide*, Zhang, Y., & Cheng, Q. (Eds.) pp. 1-31.10.5772/intechopen.100504
2. Barthel, F. & Neumayer, E. (2012). A trend analysis of normalized insured damage from natural disasters, *Climatic Change* 113(2), 215–237. <https://ssrn.com/abstract=1831633>
3. Bell, R. & Glade, T. (2004). Multi-hazard analysis in natural risk assessment. *WIT Trans on state-of-the-art in science and engineering*, 53. <https://api.semanticscholar.org/CorpusID:55274221>
4. Bordbar, M., Aghamohammadi, H., Pourghasemi, H.R. & Azizi, Z. (2022). Multi-hazard spatial modeling via ensembles of machine learning and meta-heuristic techniques. *Scientific reports*, 12, 145. Doi: 10.1038/s41598-022-05364-y
5. Breiman, L. & Cutler, A. (1993). A deterministic algorithm for global optimization. *Mathematical Programming*, 58 (1-3), 179-199. <https://doi.org/10.1007/BF01581266>
6. Cao, J., Zhang, Z., Du, J., Zhang, L., Song, Y., & Sun, G. (2020). Multi-geohazards susceptibility mapping based on machine learning - A case study in Jiuzhaigou, China. *Natural hazards*, 102 (3), 851-871. doi: 10.1007/s11069-020-03927-8
7. Chang, N.B., Parvathinathan, G. & Breeden, J.B. (2008). Combining GIS with fuzzy multi-criteria decision making for landfill siting in a fast-growing urban region. *J Environ Manage*, 87 (1), 138-153. doi: 10.1016/j.jenvman.2007.01.011
8. Chen, T. & Guestrin, C. (2016). XGBoost: A scalable tree boosting system. In *Proceedings of the 22nd ACM SIGKDD International Conference on Knowledge Discovery and Data Mining*, pp. 785-794 <https://doi.org/10.1145/2939672.2939785>
9. Cortes, C. & Vladimir, V. (1995). Support-vector networks, *Machine learning*, 20, 273-297. <https://doi.org/10.1007/BF00994018>
10. Cutter, S.L. (2018). Compound, cascading, or complex disasters: what's in a name? *Environ Sci Policy Sustain Dev*, 60 (6), 16-25. <https://doi.org/10.1080/00139157.2018.1517518>
11. Duda, R.O., Hart, P.E. & Stork, D.G. (2001). *Pattern Classification*, second edition, Wiley- Interscience, United States. P688 ISBN: 978-0-471-05669-0

12. Freund, Y. & Schapire, R.E. (1997). A Decision-Theoretic Generalization of On-Line Learning and an Application to Boosting. *J. Comput. Syst. Sci.*, 55(1), 119–139. <https://doi.org/10.1006/jcss.1997.1504>
13. Friedman, J.H. (1991). Multivariate adaptive regression splines. *The Annals of statistics*, 19 (1), 1-67 [http://www.stat.yale.edu/~lc436/08Spring665/Mars\\_Friedman\\_91.pdf](http://www.stat.yale.edu/~lc436/08Spring665/Mars_Friedman_91.pdf)
14. Friedman, J.H. (2001). Greedy function approximation: a gradient boosting machine. *Annals of Statistics*, 29(5), 1189-1232. doi: 10.1214/aos/1013203451
15. Friedman, J.H. (2002). Stochastic gradient boosting. *Computational statistics & data analysis*, 38 (4), 367-378. doi: 10.1016/S0167-9473(01)00065-2
16. GAR (2022). Global assessment report on disaster risk reduction. Our world at risk: Transforming governance for a resilient future, United Nations office for disaster risk reduction. <https://www.undrr.org/gar/gar2022-our-world-risk-gar>
17. Gevaert, C.M., Carman, M., Rosman, B., Georgiadou, Y. & Soden, R. (2021). Fairness and accountability of AI in disaster risk management: Opportunities and challenges. *Patterns*, 2 (11):100363. <https://doi.org/10.1016/j.patter.2021.100363>
18. GFDRR (2018) Machine Learning for Disaster Risk Management. Washington, DC: GFDRR. A guidance note on how machine learning can be used for disaster risk management, including key definitions, case studies, and practical considerations for implementation. [https://www.gfdr.org/sites/default/files/publication/181222\\_WorldBank\\_DisasterRiskManagement\\_Ebook\\_D6.pdf](https://www.gfdr.org/sites/default/files/publication/181222_WorldBank_DisasterRiskManagement_Ebook_D6.pdf)
19. Gill, J.C. & Malamud, B.D. (2016). Hazard interactions and interaction network (cascades) within multi-hazard methodologies. *Earth Syst. Dynam.* 7, 659-679. Doi:10.5194/esd-7-659-2016
20. Goetz, J., Brenning, A.H. & Petschko, P.L. (2015). Evaluating machine learning and statistical prediction techniques for landslide susceptibility modeling. *Comput Geosci*, 81(C), 1-11. doi: 10.1016/j.cageo.2015.04.007
21. Gruber, F.E. & Mergili, M. (2013). Regional-scale analysis of high-mountain multi-hazard and risk indicators in the Pamir (Tajikistan) with GRASS GIS. *Nat. Hazards Earth Syst Sci*, 13 (10), 2779–2796. <https://doi.org/10.5194/nhess-13-2779-2013>
22. Hastie, T. & Tibshirani, R. (1986). Generalized additive Models. *Statistical Science*, 1(3), 297-310. <http://www.jstor.org/stable/2245459>
23. He, Q., Jiang, Z., Wang, M. & Liu, K. (2021). Landslide and wildfire susceptibility assessment in Southeast Asia using ensemble machine learning methods. *Remote Sens*, 13, 1572. <https://doi.org/10.3390/rs13081572>
24. Hill, D.J. & Minsker, B.S. (2010). Anomaly detection in streaming environmental sensor data: A data-driven modeling approach. *Environ. Model. & Softw.*, 25(9), 1014-1022. doi: 10.1016/j.envsoft.2009.08.010
25. Hotelling, H. (1933). Analysis of a complex of statistical variables into principal components. *Journal of Educational Psychology*, 24 (6), 417. <https://doi.org/10.1037/h0071325>
26. Huang, X., Li, Z., Wang, C. & Ning, H. (2020). Identifying disaster-related social media for rapid response: A visual-textual fused CNN architecture. *Int J Digit Earth*, 13 (9), 1017-1039. doi: 10.1080/17538947.2019.1633425
27. IHCAP (2017). Urbanization Challenges in the Himalayan Region in the context of climate change adaptation and disaster risk mitigation; Indian Himalayan Climate Change Program, New Delhi.
28. IPCC (2021). *Summary for Policy Makers, Climate Change 2021: The Physical Science Basis*. Contribution of Working Group I to the Sixth Assessment Report of the Intergovernmental Panel on Climate Change, Masson - Delmotte, V. P., Zhai, A. et al. <https://www.ipcc.ch/report/ar6/wg1/chapter/summary-for-policy-makers/>
29. Jang, J.S. (1993). ANFIS: Adaptive-network-based fuzzy inference system. *IEEE Trans. Syst. Man Cybern*, 23 (3), 665–685. doi: 10.1109/21.256541
30. Javidan, N., Kaviani, A., Pourghasemi, H.R., Conoscenti, C., Jafarian, Z. & Rodrigo-Comino, Z.J. (2021). Evaluation of multi-hazard map produced using MaxEnt machine learning technique, *Sci Rep*, 11, 6496. <https://doi.org/10.1038/s41598-021-85862-7>
31. Kalantari, Z., Ferreira, C.S.S., Koutsouris, A.J., Ahmer, A.K., Cerdà, A. & Destouni, G. (2019). Assessing flood probability for transportation infrastructure based on catchment characteristics, sediment connectivity, and remotely sensed soil moisture. *Sci Total Environ*, 661,393–406. doi: 10.1016/j.scitotenv.2019.01.009
32. Kappes, M.S., Keiler, M. & Glade, T. (2010). From single to multi-hazard risk analysis; a concept addressing emerging challenges. In: Malet, J.P., Glade, T., Casagli, N. (ed) *Mountain Risks; Bringing Science to Society* (International conference), CERG edition, Strassbourg, France <http://cerg.eu> ISBN 2-95183317-1-5
33. Kappes, M.S., Keiler, M., Von Elverfeldt K. & Glade, T. (2012). Challenges of analyzing multi-hazard risk: A review, *Nat Hazards*, 64, 1925-1958. <https://doi.org/10.1007/s11069-012-0294-2>
34. Karlsson, C.S.J., Kalantari, Z., Mörtberg, U., Olofsson, B. & Lyon, S.W. (2017). Natural hazard susceptibility assessment for road planning using spatial multi-criteria analysis. *Environ Manag*, 60, 823–851. <https://doi.org/10.1007/s00267-017-0912-6>
35. Kennedy, J., Eberhart, R.C. (1995). Particle swarm optimization. *Proceedings of ICNN'95 - International Conference on Neural Networks*, Perth, WA, Australia, 1995, pp 1942-1948 vol 4. doi: 10.1109/ICNN.1995.488968

36. Keršulien. V. & Turskis, Z. (2011). Integrated fuzzy multiple criteria decision-making model for architect selection. *Technol. Econ. Dev. Econ.*, 17 (4), 645–666. doi:10.3846/20294913.2011.635718
37. Khatakho, R., Gautam, D., Aryal, K.R., Pandey, V.P., Rupakhety, R., Lamichhane, S., Yi- Chung Liu et al. (2021). Multi-hazard risk assessment of Kathmandu Valley, Nepal. *Sustainability*, 13(10), 5369. <https://doi.org/10.3390/su13105369>
38. Khosravi, K., Panahi, M., Bui, D.T. (2018). Spatial prediction of groundwater spring potential mapping based on an adaptive neuro-fuzzy inference system and metaheuristic optimization. *Hydrol Earth Syst Sci*, 22 (9), 4771– 4792. doi: 10.5194/hess-22-4771-2018
39. Kuglitsch, M., Arif, A., Aquino, R. et al. (2022). Artificial intelligence for disaster risk reduction: opportunities, challenges, and prospects. *World Meteorological Organization Bulletin*, 71 (1). <https://public.wmo.int/en/resources/bulletin/artificial-intelligence-disaster-risk-reduction-opportunities-challenges-and>
40. Linardos, V., Drakaki, M., Tzionas, P. & Karnavas, Y.L. (2022). Machine learning in disaster management: Recent developments in methods and applications. *Machine learning knowledge extraction*, 4 (2), 446-473. <https://doi.org/10.3390/make4020020>
41. Lloyd, S.P. (1982). Least squares quantization in PCM, *IEEE Transactions on Information Theory*, 28(2), 129–137
42. Marzban, C. (2004). The ROC curve and the area under it as performance measures, *Weather Forecast*, 19 (6), 1106–1114. doi: <https://doi.org/10.1175/825.1>
43. Michlielsen, A., Kalantari, Z., Lyon, S.W. & Liljegren, E. (2016). Predicting and communicating flood risk of transport infrastructure based on watershed characteristics. *J Environ Manag.* 182, 505–518. <https://doi.org/10.1016/j.jenvman.2016.07.051>
44. Mirjalili, S. Mirjalili, S.M. & Lewis, A. (2014). Gray Wolf optimizer. *Adv. Eng. Softw.* 69, 46–61. <https://doi.org/10.1016/j.advengsoft.2013.12.007>
45. Mukherji, A., Scott, C., Molden, D. & Maharjan, A. (2018). Megatrends in Hindu Kush Himalaya: climate change, urbanization and migration and their implications for water, energy and food. In: Biswas, A.K., Tortajada, C., Rohner, P. (ed) *Assessing Global Water Megatrends, Water Resources Development and Management*, Springer, Singapore pp 125–146. [https://doi.org/10.1007/978-981-10-6695-5\\_8](https://doi.org/10.1007/978-981-10-6695-5_8)
46. Nachappa, T.G., Ghorbanzadeh, O., Gholamnia, K. & Blaschke, T. (2020). Multi-hazard exposure mapping using machine learning for the state of Salzburg., Austria. *Remot Sens*, 12, 2757. <https://doi.org/10.3390/rs12172757>
47. Nelder, J.A. & Wedderburn, R.W.M. (1972). Generalized Linear Models. *Journal of the Royal Statistical Society, Series A (General)*, 135 (2), 370–384 <https://doi.org/10.2307/2344614>
48. Phillips, S.J., Dudík, M. & Schapire, R.E. (2021). Maxent software for modeling species niches and distributions. [http://biodiversityinformatics.amnh.org/open\\_source/maxent/](http://biodiversityinformatics.amnh.org/open_source/maxent/)
49. Pourghasemi, H.R., Gayen, A., Edalat, M., Zarafshar, M. & Tiefenbacher, J.P. (2020). Is multi-hazard mapping effective in assessing natural hazards and integrated watershed management? *Geosci Front*, 11(4), 1203-1217. <https://doi.org/10.1016/j.gsf.2019.10.008>
50. Pourghasemi, H.R., Gayen, A., Panahi, M., Rezaie, F. & Blaschke, T. (2019). Multi-hazard probability assessment and mapping in Iran. *Sci Total Environ*, 692, 556–571. doi: 10.1016/j.scitotenv.2019.07.203
51. Pourghasemi, H.R., Kariminejad, N., Amiri, M. et al. (2020). Assessing and mapping multi-hazard risk susceptibility using machine learning technique. *Scientific reports*, 10, 3203. <https://doi.org/10.1038/s41598-020-60191-3>
52. Pourghasemi, H.R., Yousefi, S., Kornejady, A. & Cerdà, A. (2017). Performance assessment of individual and ensemble data-mining techniques for gully erosion modeling. *Sci Total Environ*, 609, 764–775. doi: <https://doi.org/10.1016/j.scitotenv.2017.07.198>
53. Pouyan, S., Pourghasemi, H.R., Bordbar, M., Rehmanian, S. & Clague, J.J. (2021). A multi-hazard map based flooding, gully erosion, forest fires and earthquakes in Iran. *Scientific Reports*, 11 (1), 4889. doi: 10.1038/s41598-021-94266-6
54. Rahmati, O., Yousefi, S., Kalantari, Z. et al. (2019). Multi-Hazard exposure mapping using machine learning techniques: A case study from Iran. *Remote Sens*, 11(16), 1943. <https://doi.org/10.3390/rs11161943>
55. Ramsay, J.O. & Dalzell, C.J. (1991). Some Tools for Functional Data Analysis. *Journal of the Royal Statistical Society. Series B (Methodological)*, 53 (3), 539–572. <http://www.jstor.org/stable/2345586>
56. Rigg, J., Oven, K.J., Basyal, G.K., Lamichhane, R. (2016). Between a rock and a hard place: vulnerability and precarity in rural Nepal. *Geoforum*, 76, 63–74. <https://doi.org/10.1016/j.geoforum.2016.08.014>
57. Rocchi, A., Chiozzi, A., Nale, M. et al. (2022). Machine learning framework for multi-hazard risk assessment at the regional scale in earthquake and flood prone areas. *Appl sci*, 12, 583. <https://doi.org/10.3390/app12020583>
58. Rumelhart, D., Hinton, G. & Williams, R. (1986). Learning representations by back-propagating errors. *Nature* 323, 533–536. <https://doi.org/10.1038/323533a0>
59. Rusk, J., Maharjan, A., Tiwari, P., Chen, T.K.C., Shneiderman, S., Turin, M. & Seto, K.C. (2022). Multi-hazard susceptibility and exposure assessment of the Hindu Kush Himalaya. *Sci Total Environ*, 15,804: 150039. doi: <https://doi.org/10.1016/j.scitotenv.2021.150039>

60. Saaty, T.L. (1988). What is the Analytic Hierarchy Process? In: Mitra, G., Greenberg, H.J., Lootsma, F.A., Rijnkaert, M. J. Zimmermann, H.J. (eds) *Mathematical Models for Decision Support. NATO ASI Series, 48*, Springer, Berlin, Heidelberg. [https://doi.org/10.1007/978-3-642-83555-1\\_5](https://doi.org/10.1007/978-3-642-83555-1_5)
61. Samanta, S., Pal, D.K. & Palsamanta, B. (2018). Flood susceptibility analysis through remote sensing, GIS and frequency ratio model. *Appl Water Sci*, 8 (66), 1-14. <https://doi.org/10.1007/s13201-018-0710-1>
62. Sarker, I.H. (2021). Machine Learning: Algorithms, Real-World Applications and Research Directions. *SN Comp sci*, 2,160. <https://doi.org/10.1007/s42979-021-00592-x>
63. Schmidt, J., Matcham, I., Reese, S. et al. (2011). Quantitative multi-risk analysis for natural hazards: a framework for multi-risk modelling. *Nat Hazards*, 58 (3), 1169–1192. <https://doi.org/10.1007/s11069-011-9721-z>
64. Sharma, E. et al. (2019) Introduction to the Hindu Kush Himalaya Assessment. In Wester. P., Mishra, A., Mukherji, A. & Shrestha, A.B. (2019). (ed) *The Hindu Kush Himalaya Assessment*. Springer, Cham. [https://doi.org/10.1007/978-3-319-92288-1\\_1](https://doi.org/10.1007/978-3-319-92288-1_1)
65. Stahl, B.C. (2021). Ethical Issues of AI. In Artificial Intelligence for a better future. Springer Briefs in Research and Innovation Governance. Springer, Cham. [https://doi.org/10.1007/978-3-030-69978-9\\_4](https://doi.org/10.1007/978-3-030-69978-9_4)
66. Swets, J.A. (1988). Measuring the accuracy of diagnostic systems. *Science*, 3, (240): 1285–1293. doi: 10.1126/science.3287615
67. Tien Bui, D., Tuan, T.A., Hoang, N.D. et al. (2017). Spatial prediction of rainfall induced landslides for the Lao Cai area (Vietnam) using a novel hybrid intelligent approach of least squares support vector machines inference model and artificial Bee colony optimization. *Landslides*, 14, 447-458. doi: 10.1007/s10346-016-0711-9
68. Tuladhar, G., Yatabe, R., Dahal, R.K. & Bhandary, N.P. (2015) Disaster risk reduction knowledge of local people in Nepal. *Geoenviron Disasters*, 2 (5). <https://doi.org/10.1186/s40677-014-0011-4>
69. UN Johannesburg Plan (2002). Report of the World Summit on Sustainable Development Johannesburg, South Africa, 26 August 4 September 2002. file:///F:/Downloads/A\_CONE199\_20-EN%20(2).pdf
70. UNEP, (1992). Technical report, United Nations Environment Programme. [http://www.un.org/esa/dsd/agenda21/res\\_agenda21\\_07.shtml](http://www.un.org/esa/dsd/agenda21/res_agenda21_07.shtml)
71. UNISDR (2010). A View from the top: Vulnerability in Mountain Systems, Social Development Notes; social dimension of climate change. [https://www.unisdr.org/files/15567\\_vulnerabilitymountainsystemsune201.pdf](https://www.unisdr.org/files/15567_vulnerabilitymountainsystemsune201.pdf)
72. UNISDR (2015). HFA Decade - The Economic and Human Impact of Disasters in the Last 10 Years. [https://www.unisdr.org/files/42862\\_economichumanimpact20052014unisdr.pdf](https://www.unisdr.org/files/42862_economichumanimpact20052014unisdr.pdf)
73. Van Westen C.J. (2013). Remote sensing and GIS for natural hazards assessment and disaster risk management. In: Schroder, J.F. & Bishop, M.P. (Eds.), *Treatise on Geomorphology*, 3, pp 259-298. <https://doi.org/10.1016/B978-0-12-374739-6.00051-8>
74. Van Westen C.J. & Greiving, S. (2017). Multi-hazard risk assessment and decision making, In: *Environmental Hazards Methodologies for Risk Assessment and Management*, IWA publishing, London, UK, pp 31–94 doi: 10.2166/9781780407135\_0031
75. Wagenaar, D., Curran, A., Balbi, M. et al. (2020) Invited perspectives: how machine learning will change flood risk and impact assessment. *Natural Hazards and Earth System Sciences*, 20 (4), 1149 1161. <https://doi.org/10.5194/nhess-20-1149-2020>
76. Yousefi, S., Pourghasemi, H.R., Emami, S.N., Pouyan, S., Eskandari, S. & Tiefenbacher, J.P. (2020). A Machine learning framework for multi-hazards modeling and mapping in mountainous area. *Scientific reports*, 10 (1), 12144 doi: 10.1038/s41598-020-69233-2.
77. Youssef, A.M., Mahdi, A.M., Al-Katheri, M.M., Pouyan, S. & Pourghasemi, H.R. (2022). Multi-hazards modeling using machine learning algorithms in southwestern Saudi Arabia. *Research Square*, pp 1-33. doi: <https://doi.org/10.21203/rs.3.rs-1554302/v1>
78. Zhao, J., Zhang, Q., Wang, D. et al. (2022). Machine learning-based evaluation of susceptibility to geological hazards in the Hengduan mountains region, China. *Int J Disaster Risk Sci*, 13(1), 305-316. <https://doi.org/10.1007/s13753-022-00401-w>
79. Zschau, J. (2017). Where are we with multi-hazards, multi-risks assessment capacities? In: *Understanding disaster risk: Risk assessment methodologies and examples*. [https://drmkc.jrc.ec.europa.eu/portals/0/Knowledge/ScienceforDRM/ch02/ch02\\_subch0205.pdf](https://drmkc.jrc.ec.europa.eu/portals/0/Knowledge/ScienceforDRM/ch02/ch02_subch0205.pdf)